

Less Is More: Robust Robot Learning via Partially Observable Multi-Agent Reinforcement Learning

Wenshuai Zhao^{*†}, Eetu-Aleksi Rantala^{*‡}, Sahar Salimpour[‡], Joni Pajarinen[†], Jorge Peña-Queralta^{‡§}

[†]Department of Electrical Engineering and Automation, Aalto University, Finland.

[‡]Turku Intelligent Embedded and Robotic Systems (TIERS) Lab, University of Turku, Finland.

[§]Institute of Robotics and Intelligent Systems, ETH Zurich, Switzerland.

Emails: [†]{wenshuai.zhao, joni.pajarinen}@aalto.fi, [‡]{earant, sahars}@utu.fi, [§]{jorge.penaqueralta}@hest.ethz.ch

* These authors contributed equally to this work.

Abstract— In many multi-agent and high-dimensional robotic tasks, controllers can be optimized centrally or decentrally, using either single-agent reinforcement learning (SARL) or multi-agent reinforcement learning (MARL). However, the relationship between these two paradigms is not well-studied. This work aims to systematically investigate the robustness and performance of SARL and MARL in the same task. We first analytically show that independent Gaussian policies optimized by policy-gradient based SARL and MARL are equivalent under full-state observations. Following, we empirically show that in certain inherently single-agent tasks, perhaps surprisingly, we can use multiple agents to control a robot such that each agent only has access to partial observations. Since in these cases an agent does not depend on full state information multi-agent policies can provide additional robustness to perturbations and failures. Experiments on an illustrative decentralized control task and a mobile manipulation task with a real robot show that multiple agents with access to partial observations outperform a single agent when parts of the system fail.

Index Terms—Robot learning; Robust learning; Multi-agent reinforcement learning; Dec-POMDP; Mobile manipulation.

I. INTRODUCTION

Multi-agent reinforcement learning (MARL) provides a paradigm where multiple agents learn simultaneously and has been shown promising in simulated tasks and video games [1], [2]. Nevertheless, many existing MARL benchmark tasks can also be addressed by single-agent reinforcement learning (SARL) with a centralized controller for all the agents given full state observation [3]. Conversely, certain single-agent-like tasks may be reframed as multi-agent learning problems [4], [5]. For instance, in a classic legged-robot locomotion task, typically controlled by a centralized controller managing all joints, joints can be divided among different agents, allowing MARL algorithms to learn decentralized controllers. Despite this flexibility, the differences between these two approaches and the criteria for choosing the optimal method for new robotic tasks remain unclear.

Decentralized control has been extensively studied to achieve performance comparable to centralized control in large-scale systems [6], [7]. However, these studies often focus on mitigating the limitations of local information in decentralized controllers rather than leveraging this structure. Recent research has demonstrated that decentralized controllers for

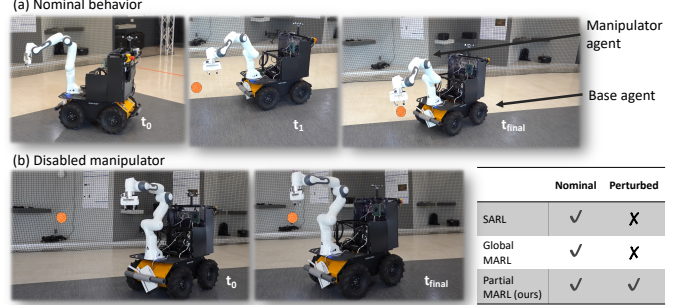


Fig. 1: Our real mobile manipulator experiments examine the robustness of learned controllers via three different methods: (i) SARL, (ii) MARL (global) and (iii) MARL (partial). In the setting shown in Figure (a), both the mobile base and the manipulator arm work normally while in (b) the manipulator is disabled to test the robustness of learned controllers. The results in different settings in the bottom right table show that although all three methods can work well with nominal behaviors, only MARL (partial) succeeds when the manipulator is disabled, demonstrating improved robustness of the controller empowered by partially observable MARL.

complex robotic systems can achieve similar or even superior performance and robustness compared to centralized controllers [8], [9], [10]. Nonetheless, these studies are typically confined to specific simulated tasks and do not provide a general investigation of design choices. In this paper, we adopt perspectives from both control theory and reinforcement learning to comprehensively explore design choices for decentralized and centralized control. We propose that multi-agent reinforcement learning (MARL) offers a flexible approach for designing decentralized controllers with local observations, potentially enhancing the robustness of robotic systems against component failures.

We start by analytically showing the equivalence between SARL and MARL under global full observation conditions. Our empirical experiments on two toy MARL tasks further indicate that MARL with limited local observations can achieve performance comparable to that with full observations. Additionally, we provide an illustrative example with proportional-integral (PI) control, highlighting the instability caused by centralized controllers with global information. Finally, in

experiments with a real-world mobile manipulation robot, our decentralized MARL controllers with local observations exhibit improved robustness to agent failure, as shown in Fig. 1. We hope this systematic investigation provides valuable insights for the design of general robotic system control.

The remainder of this document is organized as follows. Section II introduces the state of the art in MARL and robotics use cases. Section III then describes the background concepts for Dec-MDP and Dec-POMDP. We introduce the equivalence between SARNL and MARL in Section IV and empirically show the near-optimal performance of MARL agents with limited observations in Section V. Section VI provides an illustrative example to analytically show the robustness via decentralized PI controllers. Section VII describes our real robot experiments. We conclude the work and outline limitations in Section VIII.

II. RELATED WORK

We first introduce the common MARL methods and then specify works dealing with partial observation. Finally, we discuss current works using MARL for robotic tasks.

A. Multi-Agent Reinforcement Learning

Deep multi-agent reinforcement learning (MARL) has exhibited success in various game tasks [11], such as StarCraft II [2] and Stratego [12]. Value decomposition methods [13], [14] and recent multi-agent policy gradient (MAPG) methods [15], [16], [1] have demonstrated significant performance across various benchmarks [3], [5], [2]. One notable example is the Multi-agent Mujoco (*Ma-MuJoCo*) [5] domain which splits the joints of Mujoco robot tasks [17] into different agents and formulates it as a multi-agent cooperative task. Although such Mujoco tasks were traditionally used to benchmark single-agent RL methods, MARL approaches also show competitive performance. Therefore, it motivates us to investigate the connection between MARL and SARNL paradigms and their applicability to complex robotic systems.

B. Partially Observable MARL

Similar to studies in classical decentralized control theory [7], the existing literature on the partial observation problem in MARL primarily focuses on mitigating the impact of partial observation. This is typically achieved by sharing more information [18] or approximating the underlying full-state belief through various methods, such as the mean-field method [19] and agent modeling [20]. In contrast, inspired by the finding that many multi-agent learning problems can be locally independent and require only local information for near-optimal performance [6], [21], we propose leveraging the inherent structure of complex robot tasks to harness the potential of partial observation.

C. MARL for Robotics

MARL methods have been naturally used in multi-robot control tasks [22], [23], [24] due to their intrinsic decentralized control mechanism. However, some robot tasks can adopt

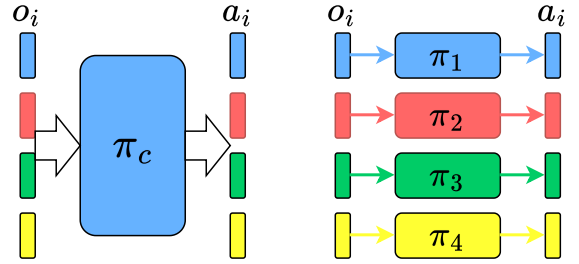


Fig. 2: Centralized controller π_c (left) with full observation vs. decentralized controllers π_i (right) with local observations.

either SARNL or MARL methods to learn controllers. For example, in bi-arm manipulation, studies such as [25] and [26] employ MARL methods to learn decentralized controllers, whereas works like [27] and recent imitation learning studies [28], [29] develop a centralized controller for all arms. Most existing works predominantly use centralized controllers for mobile manipulation [30], [31], and few studies have explored the comparative advantages of MARL over SARNL when both approaches are applicable. The closest work to ours [9] compares SARNL and MARL methods for in-hand manipulation. However, unlike our approach, they allow the decentralized controllers to observe the neighbor agents' actions, which provides critical information for the agents to adapt to malfunctions compared to SARNL baselines. In this paper, we instead seek the benefits of using less state information with MARL and comprehensively investigate the connection between SARNL and MARL.

III. PROBLEM FORMULATION

We study the fully cooperative multi-agent sequential decision-making tasks which can be formulated as a *decentralized Markov decision process* (Dec-MDP) [32] represented as a tuple $(\mathcal{S}, \{\mathcal{A}^i\}_{i \in \mathcal{N}}, r, \mathcal{P}, \gamma)$. $\mathcal{N} = \{1, \dots, n\}$ denotes a set of agents. At time step t of, each agent i observes the full state s_t in the state space \mathcal{S} of the environment and performs an action a_t^i in the action space \mathcal{A}^i from its policy $\pi^i(\cdot|s_t)$. The joint policy consists of all the individual policies $\pi(\cdot|s_t) = \pi^1 \times \dots \times \pi^n$. The environment takes the joint action of all agents $\mathbf{a}_t = \{a_t^1, \dots, a_t^n\}$, changes its state following the dynamics function $\mathcal{P} : \mathcal{S} \times \mathcal{A} \times \mathcal{S} \mapsto [0, 1]$ and generates a common reward $r : \mathcal{S} \times \mathcal{A} \mapsto \mathbb{R}$ for all the agents. $\gamma \in [0, 1]$ is a reward discount factor. The agents learn their individual policies and maximize the expected return: $\pi^* = \arg \max_{\pi} \mathbb{E}_{s, a \sim \pi, \mathcal{P}} [\sum_{t=0}^{\infty} \gamma^t r(s_t, a_t)]$. When agents only partially observe the state, the problem can be reformulated as *decentralized partially observable Markov decision process* (Dec-POMDP) [33] where agents can only access partial observation \mathcal{O}^i from the full state \mathcal{S} .

In this work, we explore the properties of controllers learned via SARNL and MARL for the same robot task. As illustrated in Fig. 2, the centralized controller π_c takes all the information and outputs all actions with one controller. By contrast, we can also design a set of decentralized controllers with different

local observations for separate action dimensions. We seek to systematically analyze and compare these two approaches for control design, from perspectives of both classical control theory and reinforcement learning.

IV. EQUIVALENCE BETWEEN SARNL AND MARL

SARNL and MARL are typically investigated independently. Here, we analytically establish their equivalence with policy gradient methods [34] under two mild assumptions. This explicit connection serves as the foundation to investigate the conditions under which they diverge and how we can leverage the unique advantages offered by MARL.

Assumption 1. *We make the following assumptions to analytically build the connection between SARNL and MARL:*

1. *Both SARNL and MARL take the full state observation;*
2. *SARNL adopts a Gaussian distribution policy with diagonal covariance for continuous action space or independent multivariate categorical distribution for discrete action space.*

The policy gradient with SARNL is estimated as follows:

$$\frac{\partial J}{\partial \theta} = \mathbb{E}_{(s, \mathbf{a}) \sim \pi} [\nabla_{\theta} \log \pi_{\theta}(\mathbf{a}|s) A(s, \mathbf{a})], \quad (1)$$

in which J is the objective we target to maximize, $J = \mathbb{E}_{(s, \mathbf{a}) \sim \pi} [\sum_{t=0}^{\infty} r_t(s, \mathbf{a})]$, and $A(s, \mathbf{a})$ denotes the advantage estimation [35]. Similarly, MARL estimates the policy gradient for each agent following:

$$\frac{\partial J}{\partial \theta^i} = \mathbb{E}_{(s, a^i) \sim \pi^i} [\nabla_{\theta^i} \log \pi_{\theta^i}(a^i|s) A(s, a^i)]. \quad (2)$$

In the Dec-MDP framework, agents share the same reward for all the interactions, and based on the first Assumption 1 of full state observation $s^i = s$, we know the value function and sample-based advantage estimation satisfy

$$V(s^i) = V(s), \text{ and } A(s^i, a^i) = A(s, \mathbf{a}) \quad (3)$$

at each time step. Based on the second Assumption 1, the joint action probability equals the product of probabilities of individual action on each dimension $\pi(\mathbf{a}|s) = \prod_{i=1}^N \pi(a^i|s)$. It is easy to get:

$$\nabla_{\theta} \log \pi_{\theta}(\mathbf{a}|s) A(s, \mathbf{a}) = \sum_{i=0}^N \nabla_{\theta} \log \pi_{\theta}(a^i|s) A(s, a^i), \quad (4)$$

which is simply the sum of the policy gradient on each agent in MARL. As such, we can conclude that the policy gradients between SARNL and MARL are mathematically equivalent under Assumption 1.

V. DOES PARTIAL OBSERVABILITY AFFECT MULTI-AGENT LEARNING?

By highlighting the aforementioned equivalence, we argue that the key advantage induced by MARL arises from flexible local observation settings for different agents. Although severe partial observation may degrade policy learning [36], in many

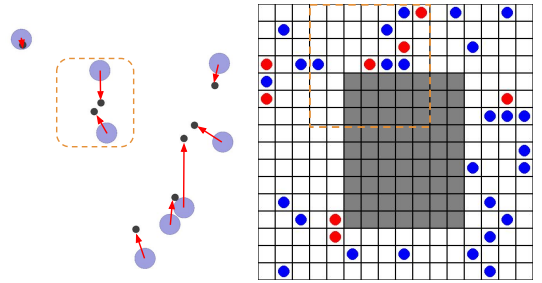


Fig. 3: Illustration of two common multi-agent tasks. **Left:** MPE *Simple-Spread* task, where 8 agents (purple circles) need to cover 8 landmarks (black dots). **Right:** *Pursuit* task where the red agents need to cooperate to surround the blue evaders. The gray block is an obstacle agents cannot traverse. The orange dashed squares in both tasks denote the partial observation range of one agent.

Dec-POMDP tasks, local observation is sufficient for near-optimal performance [37], [6], [21]. In this section, we empirically show, on two popular MARL toy tasks MPE *Simple-Spread* [38] and *Pursuit* [3], that agents are capable of making near-optimal decisions with limited local observation¹.

As shown in the left of Fig. 3, MPE *Simple-Spread* has a set of agents to cover all the landmarks as closely as possible. The shared reward is the negation of the sum of the minimum distances between each landmark and the closest agents. An additional penalty is given for collisions. In this task, each agent can only observe the velocity of its own and the relative positions of k neighborhood agents. In our experiments, we test four different amounts of closest agents that can be observed, i.e. $k \in \{2, 4, 6, 8\}$.

The *Pursuit* task shown on the right of Fig. 3 requires the pursuers (red dots) to coordinate to surround the evaders (blue dots). There are at least two agents needed to capture one evader. The agents are rewarded when any evader is successfully captured and the evader will disappear. A slight guiding reward is designed when agents tag any evader and an urgency penalty is also used to encourage agents to complete the task as soon as possible. In both tasks, the final reward is accumulated and shared by all the agents. An agent observes the information around itself in a square with a fixed size. Each square has three channels. For example, [3, 7, 7] represents the occupancy of grid cells by pursuers, evaders, and obstacles, respectively. We use three different observation ranges $k \in \{7, 10, 14\}$.

We employ multi-agent PPO (MAPPO) [1] as our policy learning method. MAPPO works in a similar way as independent PPO [16] except that MAPPO learns the critic using a concatenated global state in order to stabilize the learning process. However, during execution, the agent only uses its local observations. The learning curves are shown in Fig. 4. The consistently close performance across different observation ranges indicates that in these tasks, quite limited partial observation is sufficient to perform near-optimal decision-making. Therefore, based on this empirical evidence, we are

¹Code: <https://github.com/TIERS/partially-observable-marl>

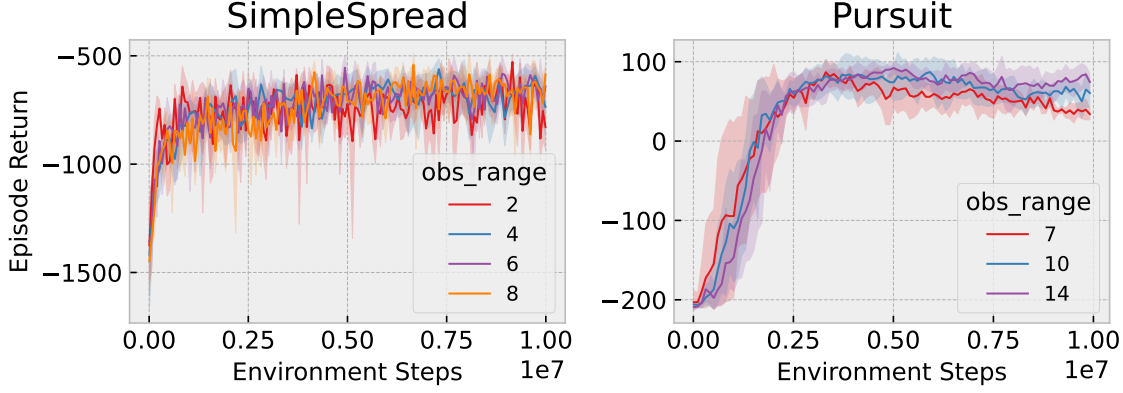


Fig. 4: Evaluation performance on MPE *Simple-Spread* (left) and *Pursuit* (right). We test different observation settings varying in $\{2, 4, 6, 8\}$ and $\{7, 10, 14\}$ in *Simple-Spread* and *Pursuit*, respectively. The performance is comparable in a relatively large range of different observation settings. We plot the average return over 5 random seeds and the shaded areas denote 95% confidence intervals.

motivated to explore the advantages equipped by partially observable MARL or decentralized control.

VI. ROBUSTNESS ARISING FROM DECENTRALIZED CONTROL

This section presents an illustrative example comparing the robustness of decentralized proportional-integral (PI) control with local observations and centralized controllers with global observations. The robustness is specifically analyzed w.r.t. system disturbances. Consider an interconnected power system [39], [7] with two generators supplying power to areas A and B, respectively. The target is to design a controller for each generator i to output power u_i to lower the power frequency deviation due to disturbance $n_i(t)$. Note that the power can be transferred between the two areas through a tie-line. Each area i follows the dynamics:

$$\begin{aligned} \frac{d(\Delta f_i)}{dt} &= -\frac{D_i}{M_i} \Delta f_i + \frac{1}{M_i} (P_i - n_i(t) \pm T_{12}(\Delta f_1 - \Delta f_2)) \\ \frac{dP_i}{dt} &= -\frac{1}{T_{g_i}} P_i + \frac{K_{g_i}}{T_{g_i}} u_i, \end{aligned}$$

where P_i and f_i denote the power generation and frequency of generator i . D_i, M_i denote the damping and inertia coefficients of Area i , while T_{g_i} and K_{g_i} denote the time constant and gain factor of a generator. We denote the tie-line power flow coefficient between Area 1 and Area 2 as T_{12} with \pm meaning minus for Area 1 while plus for Area 2. Δf_i represents the frequency deviation, whose absolute value $|\Delta f_i|$ is the objective we aim to minimize.

We compare the robustness of decentralized and centralized PI controllers. The decentralized controllers are:

$$\begin{aligned} u_1 &= -K_{d1}^P \Delta f_1 - K_{d1}^I \int_0^t (\Delta f_1) d\tau \\ u_2 &= -K_{d2}^P \Delta f_2 - K_{d2}^I \int_0^t (\Delta f_2) d\tau, \end{aligned}$$

where K^P and K^I denote the proportional gain and integral gain with the subscript di as the generator index of decentralized controller i . In contrast, centralized controllers observe frequency deviations of both generators, i.e., Δf_1 and Δf_2 . Note that the coefficients K_{c2}^P, K_{c2}^I in u_1 are non-zeros, which also applies to K_{c1}^P, K_{c1}^I in u_2 :

$$\begin{aligned} u_1 &= -K_{c1}^P \Delta f_1 - K_{c1}^I \int_0^t \Delta f_1 d\tau - K_{c2}^P \Delta f_2 - K_{c2}^I \int_0^t \Delta f_2 d\tau \\ u_2 &= -K_{c1}^P \Delta f_1 - K_{c1}^I \int_0^t \Delta f_1 d\tau - K_{c2}^P \Delta f_2 - K_{c2}^I \int_0^t \Delta f_2 d\tau, \end{aligned}$$

where K_{c1}^P represents the proportional gain of the centralized controller of generator 1 and other symbols follow the same rule. In our experiments, we only disturb Area 1 by a step function since $t = 1$, i.e., $n_1(t) = 1$ if $t \geq 1$, else 0. We do not disturb Area 2, i.e., $n_2(t) = 0$ while $t \geq 0$. The detailed hyper-parameters of each controller are left in Appendix A.

Figure 5 presents the frequency deviations of each area induced by different controllers. The results indicate that decentralized controllers significantly reduce frequency deviations. In contrast, centralized controllers introduce substantial disturbances in Δf_2 , despite Area 2 not being directly affected. This outcome is expected as the decentralized controller with local observations can naturally disregard disturbances to non-local observations, improving the decentralized controller's robustness with non-disturbed observations. It is noteworthy that this control design can be generalized to other control systems, such as modular and swarm robots, which motivates us to explore partially observable multi-agent reinforcement learning (MARL) for complex robotic systems.

VII. REAL ROBOT TASK: MOBILE MANIPULATOR REACH

This section examines the robustness of partially observable MARL on a modular real robot, where a mobile manipulator learns to reach a certain point. The mobile manipulator consists of a Clearpath Husky base (the *base agent*) and a Franka

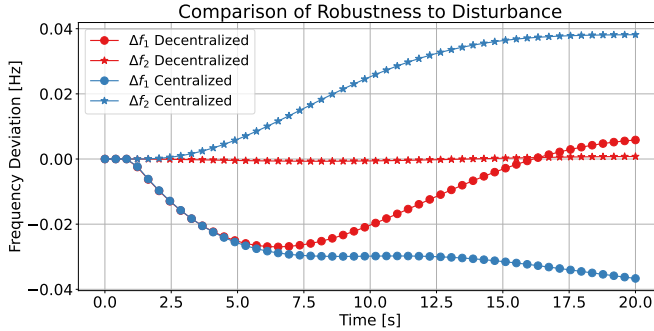


Fig. 5: Comparison of the robustness of decentralized PI controllers and a centralized PI controller on the two-area interconnected power system.

Panda 6-DoF manipulator (the *manipulator agent*), as shown in Fig. 1.

A. Experimental Setup

We consider three experimental settings to compare the different approaches in terms of SARNL vs. MARL policies, and global vs. partial observability in the MARL cases. These are (1) nominal conditions; (2) disablement of the manipulation agent; and (3) disablement of the manipulation agent with additional perturbation of its initial state. In each of the three setups, we compare a SARNL baseline with our global and partial MARL policies, all running in real time on the robots. We also set three target points at absolute positions of $\mathbf{p}_1 = (0.4, -0.6, 0.5)$, $\mathbf{p}_2 = (0.3, 2.0, 0.7)$, and $\mathbf{p}_3 = (-2.0, -1.0, 0.4)$. These are defined to force both forward and backward motions of the base, as well as rotations.

B. Task and Model Definitions

The *observation space* depends on the method. The full state information $(s_{base}, s_{arm}, s_{ee}, s_{target})$ is available for the SARNL and global MARL policies. For the partial MARL, the base agent observes $(s_{base}, s_{ee}, s_{target})$ and the mobile agent observes $(s_{arm}, s_{ee}, s_{target})$. The mobile base's state $s_{base} \in \mathbb{R}^3$ is its translation in x and y coordinates relative to the starting position of the base and its yaw in the global frame. The manipulator's state $s_{arm} \in \mathbb{R}^{18}$ is composed of its current joint angles and angular velocities of each of its joints. The manipulator's end effector's position $s_{ee} \in \mathbb{R}^3$, and the target position $s_{target} \in \mathbb{R}^3$. The positions s_{ee} and s_{target} are relative to the starting position of the base.

The *action space* for the agents are the linear and angular velocity commands for the base $(a_{base_x}, a_{base_yaw})$ and the joint commands for the manipulator $a_{arm} \in \mathbb{R}^9$ which control the desired change for the joint angles. All the actions are continuous and are clipped to a range of $[-1, 1]$.

The *reward* function is defined to minimize the distance from the end effector to the target point. For this, we use the following exponential function $r_d = \exp(-\alpha \|s_{target} - s_{ee}\|)$, where $\alpha \geq 0$ is a scalar. We also design a function r_l that penalizes joint configurations that differ excessively from the

neutral configuration to avoid reaching joint limits or destabilizing the robot. Finally, we define an additional component r_d to penalize large actions. The complete reward is then given by $r = w_d r_d - w_p r_p - w_l r_l$, with weights $w_p, w_d, w_l \geq 0$. The implementation details are available in GitHub².

C. Policy Training

We use a PPO implementation from the RLGames library which supports multiple agents [40] to train our robot policies. For *SARNL* and *global MARL* we use a single multi-layer perceptron (MLP) with separate output heads for policies and value functions. For *partial MARL*, we use two separate MLPs instead. It is worth noting that input size varies across the three methods.

The robot policy is trained in NVIDIA Isaac Sim [41], shown in Fig. 7. The simulation runs at 120Hz while the RL interaction runs at 60Hz. We set the maximum length of the episode to 500 steps. Note that all three policies are trained with the same simulation setup. The training results are shown in Fig. 8, where we can see that all three policies achieve satisfactory results and comparable returns, consistent with the multi-agent results in Section V.

D. Results

After the policy trained in Isaac Sim, we perform both *Sim-to-Real* and *Sim-to-Sim* experiments to examine the robustness of policies learned by three different methods. In *Sim-to-Real*, we deploy the learned policies to a real mobile manipulator robot and compare the robustness to perturbations and agent failure. We further extensively test the robustness on a simulated robot in Gazebo [42], as our *Sim-to-Sim* experiment. Note that the experiments are all performed without fine-tuning. In both experiments, we observe consistently improved robustness of the learned policy via partially observable MARL.

1) *Real-world*: In the real-robot experiments, the trained model weights are exported and integrated into a ROS Noetic node. The base agent controller runs in a Jetson AGX Xavier onboard computer, while the manipulator agent controller runs in an Up Xtreme board with an Intel i7 processor. Ground truth and joint poses are obtained with an Optitrack Motion Capture system. Poses are only given to the base and the arm's end effector, in addition to the target. The rest of joints representing observable states are defined only by their orientation. The experimental platform is illustrated in Fig. 9.

The experiment results are summarized in Fig. 6. In the first set of experiments with the nominal behavior of both agents as shown in Fig. 6a, the *SARNL* baseline performs the best and is able to get the closest to the target point. However, the reduced performance margin with *MARL (global)* is minimal. Importantly, even with limited observation, *MARL (partial)* reaches near-optimal performance for these experiments.

In the second set of experiments shown in Fig. 6b, we disable the *manipulator agent* entirely. The results show that *MARL (partial)* outperforms the baselines by reaching the

²Code: <https://github.com/TIERS/isaac-marl-mobile-manipulation>

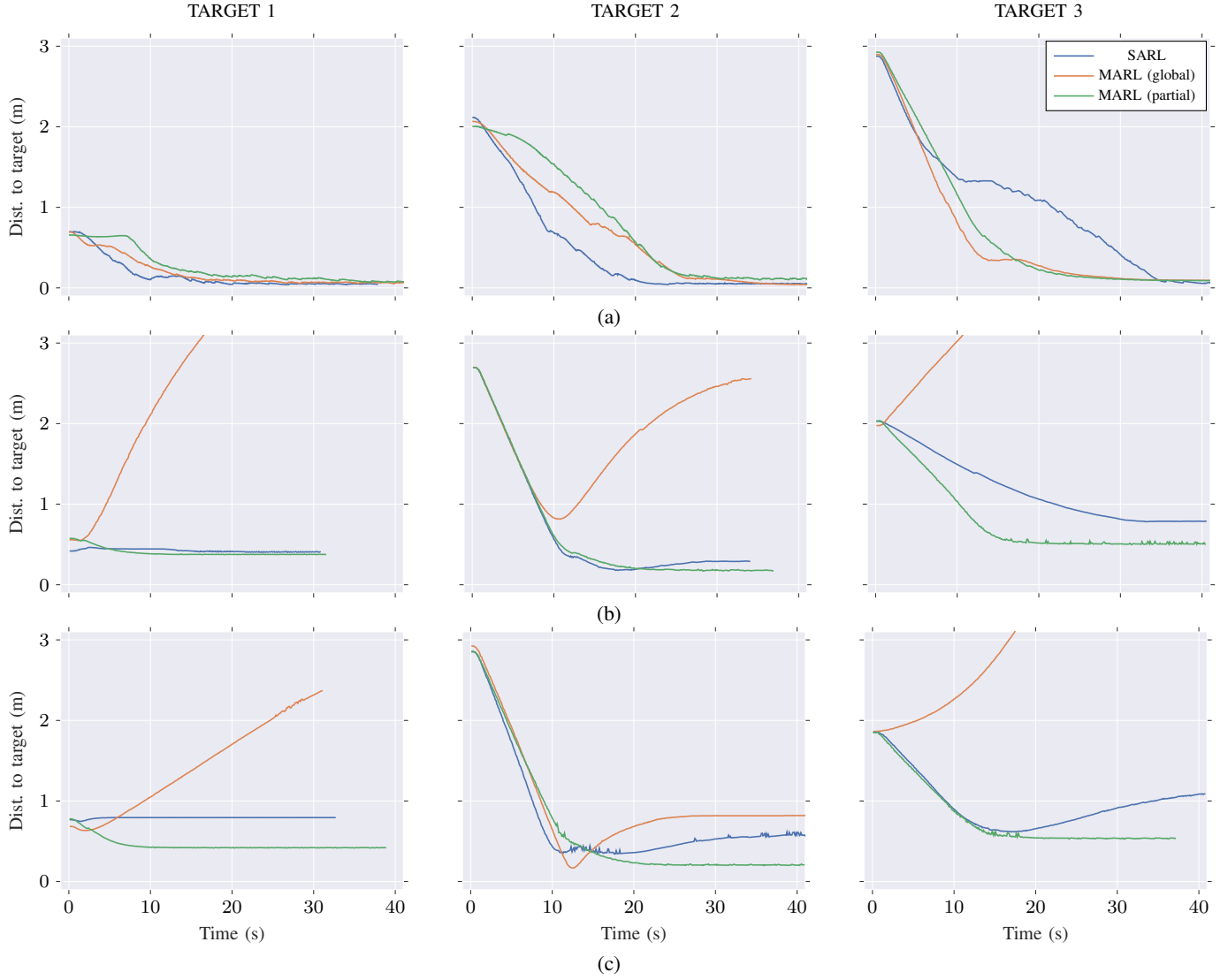


Fig. 6: Experimental results with a real-world mobile manipulator (a) under nominal conditions, (b) with the manipulator agent disabled, and (c) with the manipulator agent disabled, and also its initial position perturbed. Our experiments show all policies are able to complete the task under nominal conditions in (a). However, if one of the agents fails to move, as the manipulator in (b), the decentralized MARL approach that uses global observations for all agents fails. Finally, (c) shows that convergence is only accomplished with the partially observable MARL policy when a higher level of disturbance occurs. Therefore, our solution enables higher system robustness.

closest distances to the targets. Additionally, we observe that the *MARL (global)* baseline diverges in all three experimental trials, whereas *SARL* exhibits superior performance. We hypothesize that this disparity is due to *MARL (global)* comprising two policy networks with full state dimensions, which likely requires more data for training to reach a performance level comparable to *SARL*.

The third experiment introduces an additional perturbation to the initial state of the manipulator, resulting in a different setup from the training process. In these experiments shown in Fig. 6c, *MARL (partial)* consistently outperforms the other two baselines, with the *SARL* policy not always being able to converge. This result suggests that introducing partial observability to the agents increases the robustness to perturbations

to the system such as dysfunction of some agents.

2) *Gazebo Simulator*: Despite the real-world experiments, we thoroughly evaluate the observed results by deploying the policies on a simulated robot in Gazebo [42], as depicted in Fig. 10. Following the real-world experiments setup, we repeat each experiment 10 times using the Husky manipulation simulation package. In each repetition, we slightly randomize the target points, such that the target point is uniformly distributed within a $0.5 \times 0.5 \times 0.5 \text{ m}^3$ box. The results are summarized in Fig. 11.

In the first set of experiments with nominal agents shown in Fig. ??, all three methods achieve target points. In the second set, where the *manipulator agent* is disabled, the results mirror the real-world results: *MARL (global)* consistently diverges,



Fig. 7: Illustration of the training process in NVIDIA Isaac Sim with Isaac Gym using 512 parallel environments.

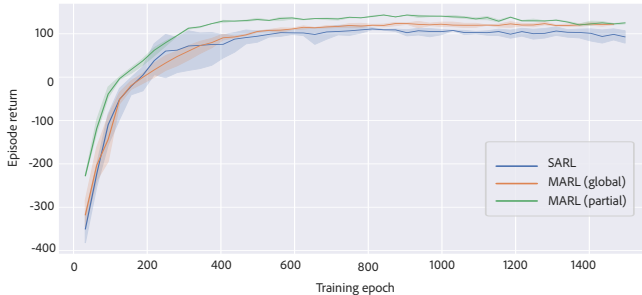


Fig. 8: Episodic returns during training using Isaac Sim.

while the *SARNL* policy demonstrates relative success across all three targets. The proposed *MARL (partial)* shows the best performance, as shown in Fig. ???. In the third set of experiments shown in Fig. ??, with an additional perturbation of the initial state of the *manipulator agent*, *MARL (partial)* is the only method that consistently succeeds.

Extensive repeated experiments conducted in the Gazebo simulation environment underscore the enhanced robustness of the tested mobile manipulator robot when employing partially observable MARL. The findings demonstrate that well-designed decentralized controllers, utilizing local observations—whether through direct control methods or learned via MARL—can offer a cheap approach to achieving superior robustness compared to centralized controllers with full observation capabilities.

VIII. CONCLUSION AND LIMITATIONS

Multi-agent reinforcement learning has arisen as a potential paradigm for controlling not only multiple, but also individual complex robots that have been previously modeled as a single agent. In this study, we comprehensively explore the potential benefits and drawbacks of MARL and SARNL control policies. We analytically examine the relationship between these two paradigms and empirically show that agents with partial observation can make near-optimal decisions. Particularly, we study



Fig. 9: Mobile manipulator used in real-world experiments with a Clearpath Husky as a base and a Panda Emika Panda manipulator.

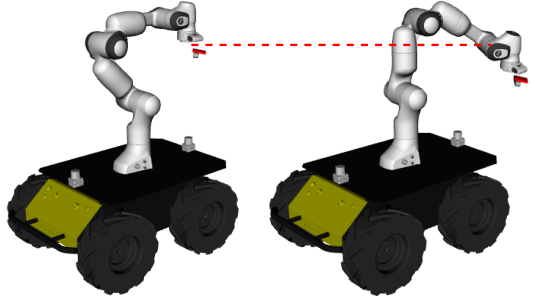


Fig. 10: The left shows the mobile manipulator in the nominal position, while the right shows the robot with a perturbed initial position. The red dashed line highlights the changed position of the end-effector.

the advantage of partially observable MARL and decentralized control. Our results on decentralized PI controllers and real-world mobile manipulator tasks indicate enhanced robustness with partial observation, which may inspire more general robust control designs.

However, our work has several limitations and offers opportunities for future improvement. First, our real-world experiments are limited in scope and could be extended to more complex tasks with critical robustness requirements. Second, it would be beneficial to formally identify the specific robot systems to which our empirical findings are applicable. Third, while we empirically demonstrate improved robustness through partial observation, there is still a need for a principled approach to designing observation spaces for decentralized controllers.

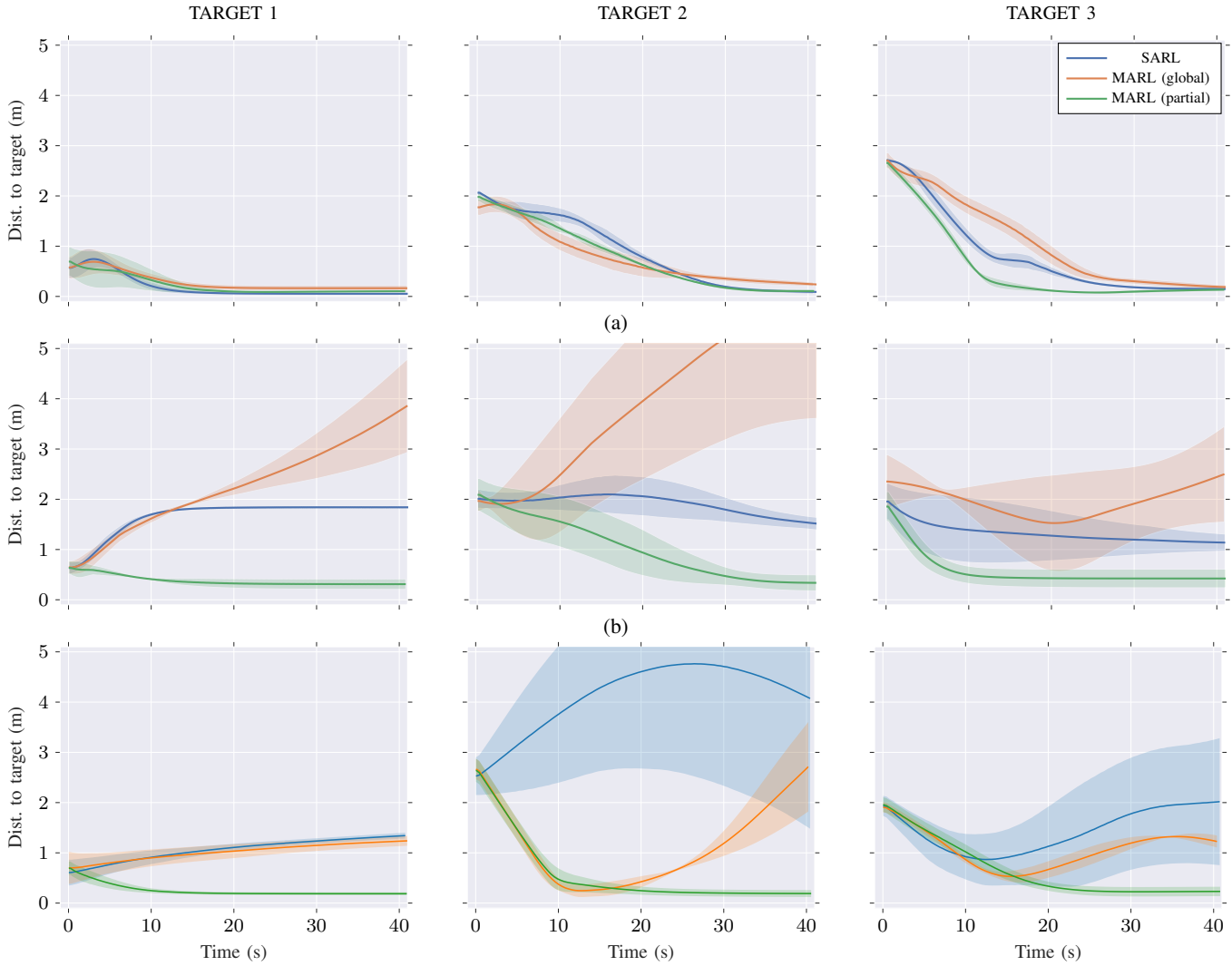


Fig. 11: *Sim-to-Sim* results in Gazebo. Experiments on each target are repeated 10 times with slightly perturbed target points. The simulated robot is experimented with (a) nominal conditions, (b) the manipulator agent disabled, and (c) the manipulator agent disabled and its initial position perturbed. Under nominal conditions (a), all policies complete the task. In (b), the MARL approach with global observations fails. And, only the partially observable MARL policy achieves convergence in (c).

APPENDIX

A. Implementation Details

The hyper-parameters used in the two-area interconnected power system are listed in Table I.

REFERENCES

- [1] C. Yu, A. Velu, E. Vinitksy, J. Gao, Y. Wang, A. Bayen, and Y. Wu, “The surprising effectiveness of ppo in cooperative multi-agent games,” *Advances in Neural Information Processing Systems*, vol. 35, pp. 24611–24624, 2022.
- [2] O. Vinyals, I. Babuschkin, W. M. Czarnecki, M. Mathieu, A. Dudzik, J. Chung, D. H. Choi, R. Powell, T. Ewalds, P. Georgiev, *et al.*, “Grandmaster level in starcraft ii using multi-agent reinforcement learning,” *Nature*, vol. 575, no. 7782, pp. 350–354, 2019.
- [3] J. Terry, B. Black, N. Grammel, M. Jayakumar, A. Hari, R. Sullivan, L. S. Santos, C. Dieffendahl, C. Horsch, R. Perez-Vicente, *et al.*, “Pettingzoo: Gym for multi-agent reinforcement learning,” *Advances in Neural Information Processing Systems*, vol. 34, pp. 15032–15043, 2021.
- [4] C. S. de Witt, B. Peng, P.-A. Kamienny, P. Torr, W. Böhmer, and S. Whiteson, “Deep multi-agent reinforcement learning for decentralized continuous cooperative control,” *arXiv preprint arXiv:2003.06709*, vol. 19, 2020.
- [5] B. Peng, T. Rashid, C. Schroeder de Witt, P.-A. Kamienny, P. Torr, W. Böhmer, and S. Whiteson, “Facmac: Factored multi-agent centralised policy gradients,” *Advances in Neural Information Processing Systems*, vol. 34, pp. 12208–12221, 2021.
- [6] J. Lavaei, “Decentralized implementation of centralized controllers for interconnected systems,” *IEEE Transactions on Automatic Control*, vol. 57, no. 7, pp. 1860–1865, 2011.
- [7] E. J. Davison, A. G. Aghdam, and D. E. Miller, *Decentralized control of large-scale systems*. Springer, 2020.
- [8] M. Schilling, K. Konen, F. W. Ohl, and T. Korthals, “Decentralized deep reinforcement learning for a distributed and adaptive locomotion controller of a hexapod robot,” in *2020 IEEE/RSJ International Conference on Intelligent Robots and Systems (IROS)*, pp. 5335–5342, IEEE, 2020.
- [9] L. Tao, J. Zhang, M. Bowman, and X. Zhang, “A multi-agent approach for adaptive finger cooperation in learning-based in-hand manipulation,” in *2023 IEEE International Conference on Robotics and Automation (ICRA)*, pp. 3897–3903, IEEE, 2023.

TABLE I: Hyper-Parameters of Interconnected Power System

Parameter	Symbol	Value
Inertia coefficient of Area 1	M_1	10
Inertia coefficient of Area 2	M_2	10
Damping coefficient of Area 1	D_1	1
Damping coefficient of Area 2	D_2	1
Time constant of generator in Area 1	T_{g1}	0.5
Time constant of generator in Area 2	T_{g2}	0.5
Gain of generator in Area 1	K_{g1}	1
Gain of generator in Area 2	K_{g2}	1
Tie-line power flow coefficient	T_{12}	0.1
Proportional gain for Area 1 (decentralized)	K_{d1}^P	1
Integral gain for Area 1 (decentralized)	K_{d1}^I	0.5
Proportional gain for Area 2 (decentralized)	K_{d2}^P	1
Integral gain for Area 2 (decentralized)	K_{d2}^I	0.5
Proportional gain for Area 1 (centralized)	K_{c1}^P	1
Integral gain for Area 1 (centralized)	K_{c1}^I	0.5
Proportional gain for Area 2 (centralized)	K_{c2}^P	1
Integral gain for Area 2 (centralized)	K_{c2}^I	0.5

[10] Y. Guo, Z. Jiang, Y.-J. Wang, J. Gao, and J. Chen, “Decentralized motor skill learning for complex robotic systems,” *IEEE Robotics and Automation Letters*, 2023.

[11] S. Gronauer and K. Diepold, “Multi-agent deep reinforcement learning: a survey,” *Artificial Intelligence Review*, pp. 1–49, 2022.

[12] J. Perolat, B. De Vylder, D. Hennes, E. Tarassov, F. Strub, V. de Boer, P. Muller, J. T. Connor, N. Burch, T. Anthony, *et al.*, “Mastering the game of stratego with model-free multiagent reinforcement learning,” *Science*, vol. 378, no. 6623, pp. 990–996, 2022.

[13] P. Sunehag, G. Lever, A. Gruslys, W. M. Czarnecki, V. Zambaldi, M. Jaderberg, M. Lanctot, N. Sonnerat, J. Z. Leibo, K. Tuyls, *et al.*, “Value-decomposition networks for cooperative multi-agent learning,” *arXiv preprint arXiv:1706.05296*, 2017.

[14] T. Rashid, M. Samvelyan, C. S. De Witt, G. Farquhar, J. Foerster, and S. Whiteson, “Monotonic value function factorisation for deep multi-agent reinforcement learning,” *The Journal of Machine Learning Research*, vol. 21, no. 1, pp. 7234–7284, 2020.

[15] J. Foerster, G. Farquhar, T. Afouras, N. Nardelli, and S. Whiteson, “Counterfactual multi-agent policy gradients,” in *Proceedings of the AAAI conference on artificial intelligence*, vol. 32, 2018.

[16] C. S. de Witt, T. Gupta, D. Makoviichuk, V. Makoviychuk, P. H. Torr, M. Sun, and S. Whiteson, “Is independent learning all you need in the starcraft multi-agent challenge?,” *arXiv preprint arXiv:2011.09533*, 2020.

[17] G. Brockman, V. Cheung, L. Pettersson, J. Schneider, J. Schulman, J. Tang, and W. Zaremba, “Openai gym,” *arXiv preprint arXiv:1606.01540*, 2016.

[18] X. Liu and K. Zhang, “Partially observable multi-agent rl with (quasi-) efficiency: the blessing of information sharing,” in *International Conference on Machine Learning*, pp. 22370–22419, PMLR, 2023.

[19] K. He, P. Doshi, and B. Banerjee, “Many agent reinforcement learning under partial observability,” *arXiv preprint arXiv:2106.09825*, 2021.

[20] G. Papoudakis, F. Christians, and S. Albrecht, “Agent modelling under partial observability for deep reinforcement learning,” *Advances in Neural Information Processing Systems*, vol. 34, pp. 19210–19222, 2021.

[21] A. DeWeese and G. Qu, “Locally interdependent multi-agent mdp: Theoretical framework for decentralized agents with dynamic dependencies,” *arXiv preprint arXiv:2406.06823*, 2024.

[22] M. Jana, L. Vachhani, and A. Sinha, “A deep reinforcement learning approach for multi-agent mobile robot patrolling,” *International Journal of Intelligent Robotics and Applications*, vol. 6, no. 4, pp. 724–745, 2022.

[23] D. L. Leottau, J. Ruiz-del Solar, and R. Babuška, “Decentralized reinforcement learning of robot behaviors,” *Artificial Intelligence*, vol. 256, pp. 130–159, 2018.

[24] W. Zhao, J. P. Queraltà, and T. Westerlund, “Sim-to-real transfer in deep reinforcement learning for robotics: a survey,” in *2020 IEEE symposium series on computational intelligence (SSCI)*, pp. 737–744, IEEE, 2020.

[25] L. Liu, Q. Liu, Y. Song, B. Pang, X. Yuan, and Q. Xu, “A collaborative control method of dual-arm robots based on deep reinforcement learning,” *Applied Sciences*, vol. 11, no. 4, p. 1816, 2021.

[26] G. Ding, J. J. Koh, K. Merckaert, B. Vanderborght, M. M. Nicotra, C. Heckman, A. Roncone, and L. Chen, “Distributed reinforcement learning for cooperative multi-robot object manipulation,” *arXiv preprint arXiv:2003.09540*, 2020.

[27] R. Chitnis, S. Tulsiani, S. Gupta, and A. Gupta, “Efficient bimanual manipulation using learned task schemas,” in *2020 IEEE International Conference on Robotics and Automation (ICRA)*, pp. 1149–1155, IEEE, 2020.

[28] T. Z. Zhao, V. Kumar, S. Levine, and C. Finn, “Learning fine-grained bimanual manipulation with low-cost hardware,” *arXiv preprint arXiv:2304.13705*, 2023.

[29] L. X. Shi, A. Sharma, T. Z. Zhao, and C. Finn, “Waypoint-based imitation learning for robotic manipulation,” *arXiv preprint arXiv:2307.14326*, 2023.

[30] N. Yokoyama, A. W. Clegg, E. Undersander, S. Ha, D. Batra, and A. Rai, “Adaptive skill coordination for robotic mobile manipulation,” *arXiv preprint arXiv:2304.00410*, 2023.

[31] C. Wang, Q. Zhang, Q. Tian, S. Li, X. Wang, D. Lane, Y. Petillot, and S. Wang, “Learning mobile manipulation through deep reinforcement learning,” *Sensors*, vol. 20, no. 3, p. 939, 2020.

[32] D. S. Bernstein, R. Givan, N. Immerman, and S. Zilberstein, “The complexity of decentralized control of markov decision processes,” *Mathematics of operations research*, vol. 27, no. 4, pp. 819–840, 2002.

[33] C. Amato, G. Chowdhary, A. Geramifard, N. K. Üre, and M. J. Kochenderfer, “Decentralized control of partially observable markov decision processes,” in *52nd IEEE Conference on Decision and Control*, pp. 2398–2405, IEEE, 2013.

[34] V. Mnih, A. P. Badia, M. Mirza, A. Graves, T. Lillicrap, T. Harley, D. Silver, and K. Kavukcuoglu, “Asynchronous methods for deep reinforcement learning,” in *International conference on machine learning*, pp. 1928–1937, PMLR, 2016.

[35] J. Schulman, P. Moritz, S. Levine, M. Jordan, and P. Abbeel, “High-dimensional continuous control using generalized advantage estimation,” *arXiv preprint arXiv:1506.02438*, 2015.

[36] Q. Liu, A. Chung, C. Szepesvári, and C. Jin, “When is partially observable reinforcement learning not scary?,” in *Conference on Learning Theory*, pp. 5175–5220, PMLR, 2022.

[37] S. Witwicki and E. Durfee, “Influence-based policy abstraction for weakly-coupled dec-pomdps,” in *Proceedings of the international conference on automated planning and scheduling*, vol. 20, pp. 185–192, 2010.

[38] R. Lowe, Y. I. Wu, A. Tamar, J. Harb, O. Pieter Abbeel, and I. Mordatch, “Multi-agent actor-critic for mixed cooperative-competitive environments,” *Advances in neural information processing systems*, vol. 30, 2017.

[39] E. Davison and N. Tripathi, “The optimal decentralized control of a large power system: Load and frequency control,” *IEEE Transactions on Automatic Control*, vol. 23, no. 2, pp. 312–325, 1978.

[40] D. Makoviichuk and V. Makoviychuk, “rl-games: A high-performance framework for reinforcement learning.” https://github.com/Denys88/rl_games, May 2021.

[41] NVIDIA, “Nvidia isaac sim.” <https://developer.nvidia.com/isaac-sim>. Accessed: 2023-09.

[42] N. Koenig and A. Howard, “Design and use paradigms for gazebo, an open-source multi-robot simulator,” in *2004 IEEE/RSJ international conference on intelligent robots and systems (IROS)(IEEE Cat. No. 04CH37566)*, vol. 3, pp. 2149–2154, Ieee, 2004.